

Independent ferroelectric contributions and rare-earth-induced polarization reversal in multiferroic TbMn₂O₅

N. Leo,^{1,2} D. Meier,³ R.V. Pisarev,⁴ N. Lee,⁵ S.-W. Cheong,⁵ and M. Fiebig*^{1,2}

¹*Department of Materials, ETH Zurich, Wolfgang-Pauli-Strasse 10, 8093 Zurich, Switzerland*

²*HISKP, Universität Bonn, Nussallee 14-16, 53115 Bonn, Germany*

³*Department of Physics, University of California, Berkeley, CA 94720, USA*

⁴*Ioffe Physical-Technical Institute, Russian Academy of Sciences, 194021 St. Petersburg, Russia*

⁵*Rutgers Center for Emergent Materials and Department of Physics & Astronomy, Rutgers, The State University of New Jersey, Piscataway, NJ 08854, USA*

(Dated: November 9, 2018)

Three independent contributions to the magnetically induced spontaneous polarization of multiferroic TbMn₂O₅ are uniquely separated by optical second harmonic generation and an analysis in terms of Landau theory. Two of them are related to the magnetic Mn^{3+/4+} order and are independent of applied fields $\mu_0 H_x$ of up to ± 7 T. The third contribution is related to the long-range antiferromagnetic Tb³⁺ order. It shows a drastic decrease upon the application of a magnetic field and mediates the change of sign of the spontaneous electric polarization in TbMn₂O₅. The close relationship between the rare-earth long-range order and the non-linear optical properties points to isotropic Tb³⁺-Tb³⁺ exchange and O²⁻ spin polarization as mechanism for this rare-earth induced ferroelectricity.

PACS numbers: 75.85.+t 77.80.-e 75.50.Ee 42.65.Ky

I. MAGNETOELECTRIC MULTIFERROICS

Materials with a coexistence of magnetic and electric long-range order, called multiferroics, exhibit a variety of remarkable magnetoelectric cross-coupling phenomena. Ferroelectric phase transitions driven by magnetic fields and magnetic phase transitions stimulated by electric fields are among the most spectacular examples. A particularly rigid coupling between magnetic and dielectric properties is obtained in multiferroics where the magnetic order induces an improper ferroelectric polarization [1–3]. Such magnetically induced ferroelectrics represent an outstanding class of multiferroics because they combine two desirable aspects: (i) A unique control of spin-based properties by electric fields, and (ii) a matchless versatility regarding intrinsic magnetoelectric coupling mechanisms. Prototypical examples are TbMn₂O₅, TbMnO₃, and CuCrO₂ in which the spontaneous polarization is attributed to magnetostrictive (exchange-symmetric), Dzyaloshinskii-Moriya-type (exchange-antisymmetric), and orbital interactions, respectively [4–6].

A characteristic feature of the magnetically induced ferroelectrics is their complexity. Various mechanisms, demanding in themselves, cooperate for promoting the spontaneous polarization: geometric frustration, incommensurate spin order, low crystallographic symmetry, and electronic $3d - 4f$ interactions may all play a role. This inevitably results in rich magnetoelectric phase diagrams with a multiplicity of contributions to the ferroelectric polarization P . The situation culminates in compounds like TbMn₂O₅ which hosts three magnetic subsystems and five different magnetically ordered phases. This leads to a complex temperature- and field-dependence of the magnetically induced polarization,

including a sign change of P induced by a moderate magnetic field [3]. Phenomenological two- and three-polarization models were proposed to explain such features and the $3d - 4f$ interplay of the manganese and the terbium sublattices was scrutinized [7, 8]. However, up to now an explicit disentanglement of individual contributions to the net polarization has not been accomplished because pyroelectric current measurements, the standard technique for measuring values in the order of 1 nC/cm², can only reveal the spatially integrated net polarization. However, a unique experimental separation of the polarization contributions and their respective magnetic-field dependence would be highly valuable for identifying the origin of magnetoelectric phase control in compounds like TbMn₂O₅.

Here we report that the spontaneous ferroelectric polarization in TbMn₂O₅ is composed of *three* independent contributions. Two of these are related to the magnetic order of the Mn^{3+/4+} ions while the third contribution originates in the antiferromagnetic Tb³⁺ order, possibly involving isotropic exchange and O²⁻ spin polarization by the rare-earth order. We show that the magnetic-field-induced change of sign of the polarization in TbMn₂O₅ is dominated by the field-induced suppression of the Tb³⁺-related polarization contribution (by to field-induced quenching of the rare-earth order) and the emergence of an oppositely polarized contribution (related to the quadratic magnetoelectric effect). In contrast, a response of the manganese-related polarizations to the magnetic field is not observed, which is corroborated by supplementary studies on isostructural YMn₂O₅. The sublattice polarizations in TbMn₂O₅ are disentangled by temperature- and magnetic-field dependent optical SHG and agree with a multi-dimensional order parameter description by Landau theory.

	T_i	\mathbf{k}	P_{net}^y
I	$T < T_1 = 43$ K	$(k_x, 0, k_z)$	–
II	$T < T_2 = 38$ K	$(0.5, 0, k_z)$	P_I^y
III	$T < T_3 = 33$ K	$(0.5, 0, 0.25)$	
IV	$T < T_4 = 24$ K	$(k_x, 0, k_z)$	$P_I^y - P_{II}^y$
V	$T < T_5 = 10$ K		$P_I^y - P_{II}^y + P_{III}^y$

TABLE I. Sequence of phase transitions in TbMn_2O_5 in zero magnetic field. T_i : transition temperatures, \mathbf{k} : magnetic propagation vector, P_{net}^y : magnetically induced net polarization composed of the contributions $P_{I,II,III}^y$. Values for T_i and \mathbf{k} were taken from Ref. 23.

It was initially proposed in Ref. 9 that three independent contributions might constitute the spontaneous ferroelectric polarization of TbMn_2O_5 . However, the separation was done in a purely phenomenological way. For demonstrating that a separation of sublattice polarizations is possible in a unique way an analysis in terms of the Landau formalism [10–12] is indispensable. In addition, attempts to clarify the relation of the sublattice polarizations to the magnetically induced change of sign of the polarization in TbMn_2O_5 were not made in Ref. 9 where all measurements were done in the absence of magnetic fields.

II. MULTIFERROIC TbMn_2O_5

The isostructural RMn_2O_5 compounds ($R^{3+} = \text{Y}$, rare earth, Bi) crystallize in the orthorhombic space group $Pbam$ (with the Cartesian x , y , and z axis corresponding to the orthorhombic a , b , and c axis, respectively). Frustrated magnetic interactions between the Mn^{3+} and Mn^{4+} ions lead to commensurate and incommensurate magnetic phases. In zero magnetic field, two successive transitions to an antiferromagnetic (AFM) and to a multiferroic state, respectively, occur around 40 K in all compounds. Additional magnetic transitions, in particular in compounds in which R represents a rare-earth element, were reported. In this Section we discuss the magnetic and multiferroic phases of TbMn_2O_5 at zero magnetic field in detail and relate them to the corresponding description by Landau theory in Ref. 10. The sequence of electric and magnetic phase transitions is summarized in Table I.

In TbMn_2O_5 , incommensurate AFM $\text{Mn}^{3+/4+}$ order in the xy plane described by the propagation vector $\mathbf{k} = (\frac{1}{2} + \delta_x, 0, \frac{1}{4} + \delta_z)$ emerges at the Néel temperature $T_N \equiv T_1 = 42$ K. The four-dimensional irreducible representation associated with \mathbf{k} leads to a ferroelectric polarization P_{net}^y along the y axis when δ_x becomes zero in a second-order phase transition at $T_C \equiv T_2 = 38$ K. Landau theory predicts a temperature dependence of the polarization according to

$$P_{\text{net}}^y(T_2 > T > T_3) = \tilde{P}_I^y(T) \propto \sqrt{T_2 - T}. \quad (1)$$

In a subsequent second-order phase transition at $T_3 = 33$ K commensurate magnetic lock-in with $\delta_x = \delta_z = 0$ occurs. The predicted temperature dependence of the ferroelectric polarization is now described by the expression

$$P_{\text{net}}^y(T_3 > T > T_4) = P_I^y(T) \propto \sqrt{T_2 - T} + \varepsilon. \quad (2)$$

Here, ε is a constant responsible for a change of slope of $P_{\text{net}}^y(T)$ at T_3 . In a first-order phase transition at $T_4 = 22$ K the magnetic order of TbMn_2O_5 becomes incommensurate again with $\delta_x \neq 0$, $\delta_z \neq 0$. The first-order phase transition is parametrized by the emergence of now two four-dimensional order parameters whose coupling gives rise to an additional polarization contribution P_{II}^y with

$$P_{II}^y(T) \propto (T_4 - T). \quad (3)$$

Because of the pronounced decrease of P_{net}^y observed at T_4 the net polarization is expressed as

$$P_{\text{net}}^y(T < T_4) = P_I^y(T) - P_{II}^y(T) = \varepsilon_1 \sqrt{T_2 - T} + \varepsilon - \varepsilon_2 (T_4 - T) \quad (4)$$

with $\varepsilon_{1,2}$ as proportionality factors. Finally, a second-order magnetic phase transition is observed at $T_5 \approx 10$ K. The transition is associated to the long-range AFM order of the Tb^{3+} moments with the same propagation vector as for the $\text{Mn}^{3+/4+}$ moments [14, 15]. It is accompanied by a recovery of the ferroelectric net polarization. Hence, a dome-like temperature dependence of P_{II}^y or, alternatively, a third contribution P_{III}^y to the net polarization were proposed [3, 9].

III. OPTICAL SECOND HARMONIC GENERATION (SHG)

Optical SHG describes the induction of a light wave at frequency 2ω by an incident light wave at frequency ω [16, 17]. This is expressed as $S_i(2\omega) = \epsilon_0 \chi_{ijk} E_j(\omega) E_k(\omega)$. The component χ_{ijk} of the corresponding non-linear susceptibility tensor couples j and k polarized contributions of the incident light field $\mathbf{E}(\omega)$ to an i polarized contribution of the SHG source term $\mathbf{S}(2\omega)$. The according SHG intensity is $I_{ijk} \propto |\mathbf{S}(2\omega)|^2 \propto |\chi_{ijk}|^2$. In the electric-dipole approximation $\hat{\chi}$ is a polar tensor with $\hat{\chi} \neq 0$ in non-centrosymmetric systems only [16]. Thus, SHG is well suited for detecting ferroelectric order breaking the inversion symmetry [18]. Moreover, contrary to linear optical techniques, the ferroelectric SHG contribution emerges free of background. In addition, the polarization of the light waves at ω and 2ω that are involved in the SHG process reveals the symmetry and orientation of the ferroelectric order parameter, i.e., the direction of the spontaneous polarization.

An analysis of the spectral dependence of the SHG signal reveals the electronic states contributing to the local electric-dipole moment and, hence, to the macroscopic

polarization. Thus, independent contributions to the ferroelectric polarization can be separated by measurements of the SHG signal in dependence of the polarization of the light fields, photon energy, temperature and magnetic field.

IV. EXPERIMENTAL SETUP

SHG was measured with 5-ns laser pulses using the transmission setup described elsewhere [9, 17]. We used (100)-oriented TbMn_2O_5 and YMn_2O_5 samples with a thickness of 50 and 100 μm , respectively, which were polished with a silica slurry. The samples were mounted in a temperature-tunable liquid-helium-operated cryostat for fields up to 7 T (Oxford Spectromag SM4000). The magnetic field was applied in the Faraday configuration ($\mathbf{H} \parallel x$). The integrated SHG intensity of the sample was measured while heating it (heat rate 0.5 – 1 K/min) or sweeping the magnetic field (sweep rate 0.25 – 0.5 T/min). An electric single-domain poling procedure was omitted because even in zero electric field the samples were found to predominantly form a ferroelectric single-domain state.

V. CONTRIBUTIONS TO THE ZERO-FIELD NET POLARIZATION

We first present measurements at zero magnetic field in order to demonstrate the method of separating independent contributions to the ferroelectric net polarization and verify the consistency between the temperature dependence of these contributions and the behaviour expected from Landau theory.

Figure 1 shows the temperature dependence of the SHG signals I_{yyy} and I_{zyz} in TbMn_2O_5 at $2\hbar\omega=2.08$ eV. These non-linear intensities were chosen because they allow a unique distinction of polarization contributions [9]: SHG from χ_{yyy} is present below $T_2 \approx 38$ K which marks the emergence of the magnetically induced polarization. Note that the temperature dependence of $\sqrt{I_{yyy}} \propto |\chi_{yyy}|$ resembles pyroelectric current measurements of the net polarization [3, 19]. In contrast, I_{zyz} is non-zero only below the first-order commensurate-to-incommensurate transition at $T_4 \approx 22$ K. Thus, at least two independent contributions to the net polarization are present which correspond to separate SHG light fields interfering in a different way in Figs. 1(a) and 1(b).

We now apply a systematic fit procedure employing the temperature dependence as predicted by Landau theory [10] in Section II. For $T_2 \geq T > T_4$ the intensity I_{yyy} depends only on the polarization $P_I^y(T)$ according to Eqs. (1) and (2) in good agreement with the fit in Fig. 1(a). For $T_4 \geq T \geq T_5$ the additional polarization P_{II}^y is present. In this temperature range I_{zyz} in Fig. 1(b) couples solely to P_{II}^y and reveals the relation $I_{zyz} \propto T^2$ expected from Eq. (3). In contrast, I_{yyy} in-

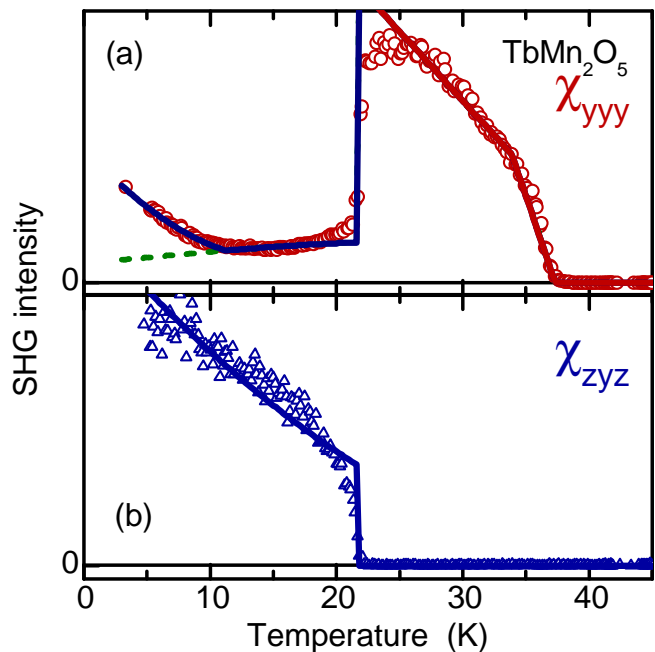


FIG. 1. (Color online) Separation of sublattice polarizations in TbMn_2O_5 . Temperature dependence of the SHG contributions $I_{ijk} \propto |\chi_{ijk}|^2$ for (a) χ_{yyy} and (b) χ_{zyz} measured in the same experimental run at $2\hbar\omega=2.08$ eV in zero magnetic field. Three independent contributions $P_{I,II,III}^y$ to the net polarization are uniquely distinguished (see text). Whereas χ_{yyy} in (a) couples to a coherent superposition of all three sublattice polarizations, χ_{zyz} in figure (b) couples exclusively to the polarization $P_{II}^y(T)$. Lines are fits in agreement with Landau theory (Eqs. 1 to 7) as explained in Section V. Note that the data below 10 K in (a) cannot be explained by a sum of P_I^y and P_{II}^y (dashed line), so that a third contribution, P_{III}^y , related to the magnetic order of the Tb^{3+} ions has to be taken into account (solid line).

cludes interfering SHG contributions from P_I^y and P_{II}^y . This is described by

$$I_{yyy}(T_4 \geq T \geq T_5) = I_0 |P_I^y(T) + Ae^{i\phi} P_{II}^y(T)|^2 \quad (5)$$

Here, $P_{I,II}^y(T)$ are derived by fitting Eqs. (1) to (3), respectively, in the temperature range where they constitute the only contribution to the SHG signal: (i) $P_I^y(T)$ is derived by fitting Eqs. (1) and (2) to $I_{yyy}(T)$ in the range $T_4 < T \leq T_2$. (ii) $P_{II}^y(T)$ is derived by fitting Eq. (3) to $I_{zyz}(T)$ for $T \leq T_4$. For fitting Eq. (5) to $I_{yyy}(T \leq T_4)$, where P_I^y and P_{II}^y interfere, the relative amplitude A and the phase ϕ were varied whereas $P_{I,II}^y$ were adopted from the fits in (i) and (ii). For $T \geq T_5$ the fits leads to a good agreement between data and theory in Fig. 1 except near T_4 . Here, the change of the SHG intensity is smeared out due to the abrupt nature of the first-order transition and because of a thermal gradient across the sample caused by laser heating. This also leads to small deviation between the transition temperatures $T_{2,3,4}$ obtained here and their literature values [3, 20].

Below $T_5 \approx 10$ K Eq. (5) fails to describe the tem-

perature dependence of the SHG data in Fig. 1(a) which indicates the presence of a *third* contribution to the net polarization of TbMn_2O_5 . The value of T_5 shows that the long-range order of the Tb^{3+} lattice is responsible for this contribution. Hence, the corresponding ferroelectric polarization P_{III}^y is improper so that the temperature dependence has to scale linearly according to Landau theory:

$$P_{III}^y(T) \propto (T_5 - T). \quad (6)$$

In an extension of Eq. (5) the corresponding net SHG intensity is described by

$$I_{yyy}(T < T_5) = I_0 |P_I^y(T) + Ae^{i\phi} P_{II}^y(T) + A'e^{i\phi'} P_{III}^y(T)|^2. \quad (7)$$

For this fit only the amplitude A' and phase ϕ' were varied whereas all the other values were taken from the fit of Eq. (5) for $T_4 \geq T \geq T_5$. As Fig. 1 shows, this leads to an excellent agreement with the SHG data down to the lowest experimentally accessed temperature of about 3 K.

We thus conclude that SHG allows us to decompose the spontaneous ferroelectric net polarization of TbMn_2O_5 in a unique way into three independent sublattice polarizations $P_{I,II,III}^y$. All three contributions couple linearly to the SHG susceptibility and exhibit the temperature dependence that is expected from Landau theory. The critical temperatures at which the sublattice polarizations emerge relate P_I^y and P_{II}^y to the magnetic order of the $\text{Mn}^{3+/4+}$ lattices and the “new” contribution P_{III}^y to the AFM order of the Tb^{3+} lattice. The macroscopic net polarization is conveniently written as

$$P_{\text{net}}^y(T) = P_I^y(T) - P_{II}^y(T) + P_{III}^y(T). \quad (8)$$

This reflects the antiparallel orientation of $P_I^y(T)$ and $P_{II}^y(T)$ which is responsible for the pronounced decrease of $P_{\text{net}}^y(T)$ at T_4 .

VI. MAGNETIC-FIELD DEPENDENCE OF THE POLARIZATION

After establishing the relation between the SHG signal and the ferroelectric net polarization in TbMn_2O_5 we now investigate the response of the SHG yield to a static magnetic field applied along the x axis. Figures 2(a) and 2(b) show the temperature dependence of I_{yyy} and I_{zyz} for magnetic fields $\mu_0 H_x$ of 0, 3, and 7 T. The most pronounced effects of the magnetic field are the shift [3, 20] of the first-order transition temperature T_4 and the suppression of I_{yyy} below this temperature.

We now apply the same step-by-step analysis as in Section V with consecutive derivation of P_I^y , P_{II}^y , and P_{III}^y and the associated fit parameters according to Eq. (7). For this purpose, Fig. 3 shows the magnetic-field dependence of I_{yyy} and I_{zyz} at fixed photon energies and temperatures. The SHG signals in Figs. 3(a) and 3(b) are

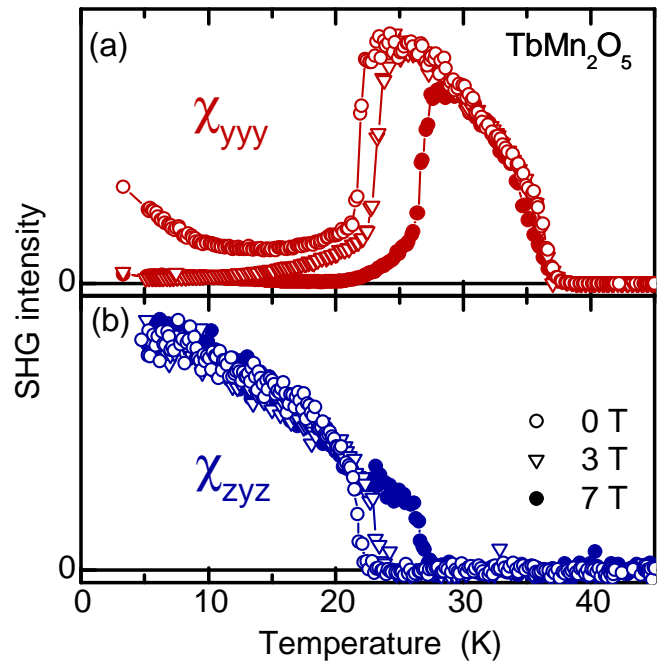


FIG. 2. (Color online) Temperature dependence of the SHG contributions from (a) χ_{yyy} and (b) χ_{zyz} measured in the same experimental run at $2\hbar\omega=2.08$ eV at different magnetic fields $\mu_0 H_x$. Note the suppression of χ_{yyy} at low temperatures (a) and the shift of the first-order transition temperature from 22 K to 27 K (a,b). In spite of this shift the amplitude of neither χ_{yyy} above 30 K (in (a)) nor of χ_{zyz} (in (b)) show a magnetic-field dependence.

constant across the whole range of the magnetic-field. As shown in Section V, I_{yyy} at 30 K and 2.08 eV couples solely to P_I^y whereas I_{zyz} at 20 K and 2.08 eV is only determined by P_{II}^y . We therefore conclude that, although the commensurate phase is notably stabilized by the magnetic field (see the shift of the first-order-transition temperature in Fig. 2(a) and Refs. 3 and 20), the absolute values of the polarizations P_I^y and P_{II}^y are *not affected* by fields up to ± 7 T. Consequently, the pronounced magnetoelectric response in TbMn_2O_5 must be *solely* due to the rare-earth induced polarization contribution. This is corroborated in an impressive way by SHG data on YMn_2O_5 which are shown in Fig. 4: The temperature dependence of I_{yyy} and I_{zyz} is similar to that of TbMn_2O_5 and allows us to distinguish the sublattice polarizations P_I^y and P_{II}^y according to Eqs. (1) to (5). However, contributions from P_{III}^y are absent because of the diamagnetic Y^{3+} sublattice. Along with this, the data in Fig. 4 display no dependence on the applied magnetic field aside from a small shift of the first-order-transition temperature T_4 . The role of P_{III}^y in TbMn_2O_5 is highlighted in Fig. 3(c) which shows $I_{yyy}(H_x)$ at 7 K and 2.08 eV. The SHG signal displays minima at ± 3 T and a steady increase of the SHG intensity away from this value. Because of the independence of $P_{I,II}^y$ on magnetic field Fig. 3(c) directly reflects the magnetic-field depen-

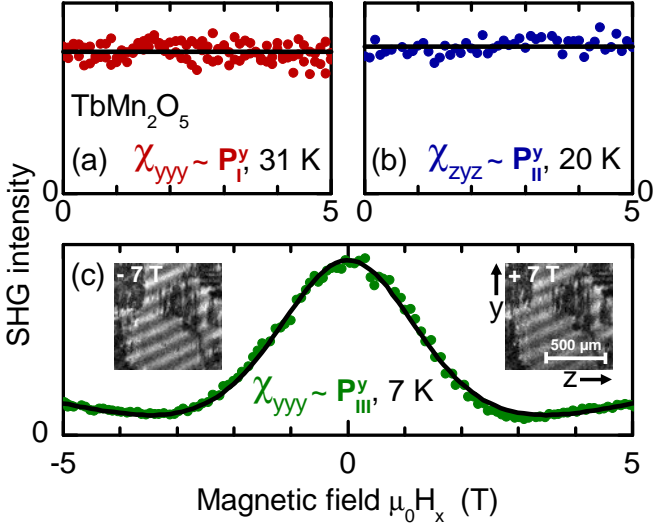


FIG. 3. (Color online) Magnetic field dependence of the sublattice polarizations of TbMn_2O_5 : SHG from (a) χ_{yyy} at 31 K and (b) χ_{zyz} at 20 K for $2\hbar\omega=2.08$ eV while sweeping the magnetic field $\mu_0 H_x$. These contributions couple to the $\text{Mn}^{3+/4+}$ -related polarizations P_I^y and P_{II}^y , respectively, and do not display a magnetic-field dependence. (c) SHG from χ_{yyy} at low temperatures. This contribution couples to the Tb^{3+} -related polarization P_{III}^y and displays a pronounced magnetization dependence. The solid line represents a fit to Eq. (9) to the data. Insets in (c) show that the ferroelectric domain structure is independent of the applied magnetic field. Insets show spatially resolved SHG images of TbMn_2O_5 for χ_{yyy} at 2.08 eV and 5 K in fields of -7 T and $+7$ T, respectively. Note that the position of the ferroelectric domains and domain walls (dark regions) does not change in the course of the magnetic field reversal. (The periodic overall variation of brightness are interference fringes of the fundamental light in the sample.)

dence of P_{III}^y . The symmetric shape of I_{yyy} reveals that there is no hysteresis. In addition, the response is independent of the sign of H_x which indicates a quadratic field-dependence of $P_{III}^y(H_x)$. An expression taking these observations into account is

$$P_{III}^y(T, H_x) = P_{III}^y(T, 0) - \beta M_x^2(T, H_x). \quad (9)$$

Here we assume that, as discussed below, the alignment of the large magnetic moment of the $\text{Tb}^{3+}(4f^8)$ ions leads to a magnetization described by a Brillouin function according to $M_x \propto B_J(T, H_x)$ with $J = 6$ and $g_J = 1.5$ for Tb^{3+} . The data in Fig. 3(c) can now be fitted by Eq. (7) into which we enter $P_{III}^y(H_x)$ according to Eq. (9) as well as the field independent polarizations $P_{I,II}^y$. We see that the agreement between the SHG data and the fit is excellent.

Figure 5 shows the resulting field- and temperature-dependent decomposition of $P_{\text{net}}^y(T, H_x)$. The magnetic-field-induced change of sign of the polarization at low temperatures [3] reveals itself as the suppression and zero crossing of a single contribution, P_{III}^y , to the net polarization. Therefore, this process should not be termed

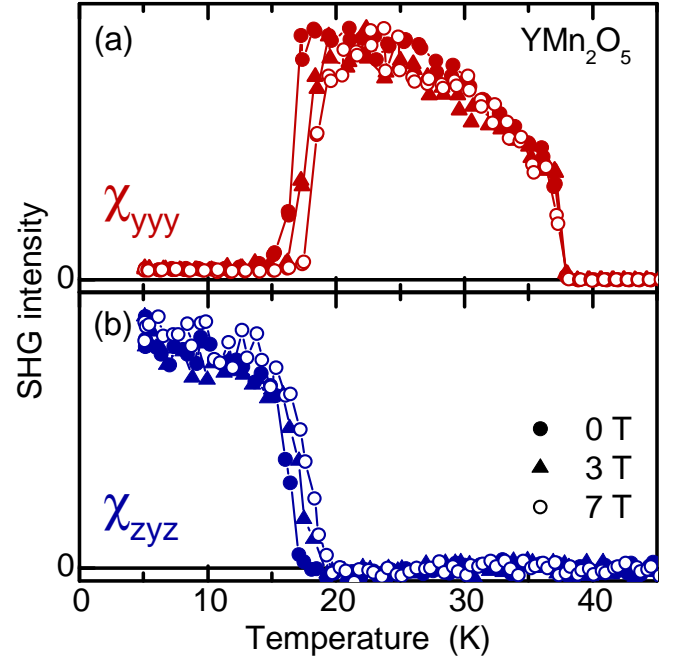


FIG. 4. (Color online) Magnetic-field dependence of sublattice polarizations in YMn_2O_5 . (a,b) Temperature dependence of the SHG contributions from (a) χ_{yyy} and (b) χ_{zyz} measured in the same experimental run at $2\hbar\omega=2.08$ eV at different magnetic fields $\mu_0 H_x$. Like in TbMn_2O_5 , two contributions to the polarization, P_I^y and P_{II}^y , can be distinguished. However, in contrast to Fig. 2 the rare-earth contribution below 10 K is absent.

“polarization reversal” or “polarization switching”, because these terms are associated to the change of polarization between $+P$ and $-P$ involving a hysteresis with the formation and movement of domains. In TbMn_2O_5 only the balance between competing contributions to the net polarization is shifted whereas the domain structure reveals small or no changes according to our SHG imaging experiments (see Fig. 3 (c)).

VII. DISCUSSION: MICROSCOPIC MECHANISMS

The essential benefit of the SHG experiments is that they allow us to separate independent contributions to the magnetically induced ferroelectric polarization in TbMn_2O_5 in a unique way and investigate their respective response to a static magnetic field. As we will see now, this leads to clues about the microscopic origin of these polarizations and of the magnetically induced change of sign of the polarization.

Experimentally we distinguish three contributions to the net polarization: The first two, P_I^y and P_{II}^y , are associated to the magnetic order of the $\text{Mn}^{3+/4+}$ sublattices. They maintain an antiparallel orientation, leading to a sudden drop of the net polarization once P_{III}^y appears at

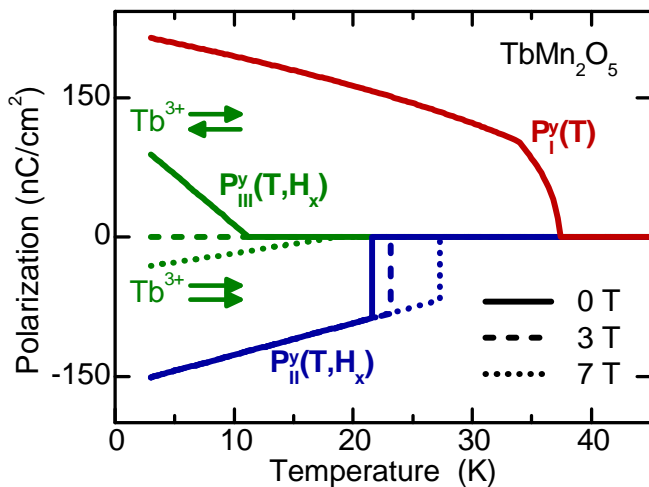


FIG. 5. (Color online) Temperature- and magnetic-field-dependent decomposition of the magnetically induced polarization $P_{\text{net}} \parallel y$ in TbMn_2O_5 . The polarizations P_I^y and P_{II}^y induced by the manganese spin order are field-independent (apart from the shift of the first-order-transition temperature T_4). These contributions are also present in YMn_2O_5 (see Fig. 4). The Tb^{3+} -related polarization contribution P_{III}^y in zero field is induced by the AFM long-range order of the rare-earth moments. In an applied magnetic field $H \parallel x$ this contribution is suppressed due to the paramagnetic magnetization of the Tb^{3+} moments whereas another field-induced contribution (related to the quadratic magnetoelectric effect) emerges. Both effects lead to the magnetic-field induced sign change of P_{net} as observed in Ref. 3.

T_4 . This was assumed before but here the separate observation of P_I^y and P_{II}^y provides an unambiguous confirmation of their opposite sign. In addition, the observation of two independent contributions rules out the model explaining the polarization drop at T_4 as transition from a ferroelectric state for $T < T_4$ to a ferrielectric state for temperatures above T_4 [21]. The magnitudes of P_I^y and P_{II}^y respond neither to magnetic fields $\mu_0 H_x$ of up to ± 7 T nor to the magnetic order of the Tb^{3+} sublattice [20]. For P_I^y this has been seen previously in the restricted temperature range $T > T_4$ where only P_I^y contributes to the net polarization. Now the SHG data in Fig. 2 give direct access to P_I^y and P_{II}^y across the entire temperature range. In contrast to field and temperature dependent pyroelectric current measurements [7], which revealed changes in the order of 10%/T, the field dependent SHG data of $P_{I,II}^y$ at fixed temperature (Figs. 3(a) and (b)) reveal no dependence on the magnetic field (with a noise level of the SHG data below 1%). It is quite remarkable that the absolute values of P_I^y and P_{II}^y are field independent although the magnetic field stabilizes the incommensurate phase ($\sim P_{II}^y$) against the commensurate phase ($\sim P_I^y$) at T_4 .

The third contribution to the net polarization, P_{III}^y , is associated to the magnetic order of the Tb^{3+} ions. This is the most interesting contribution because it is

the only one displaying a magnetic-field dependence and is therefore exclusively responsible for the magnetic-field-induced change of sign of the net polarization [3]. First of all, we see that the emergence of P_{III}^y in zero magnetic field is associated to a *specific component* of the magnetic Tb^{3+} order. We have to distinguish (i) the magnetic order exerted onto the Tb^{3+} ions by the ordered $\text{Mn}^{3+/4+}$ spins, and (ii) the magnetic order resulting from isotropic Tb^{3+} - Tb^{3+} exchange [22]. Contribution (i) is observed in the whole temperature range below T_1 [15, 23, 24]. Contribution (ii) is present below T_5 and distinguished from contribution (i) by a small characteristic hump in the dielectric resonance [14, 19]. The emergence of P_{III}^y at T_5 clearly relates it to the contribution (ii): the AFM order inherent to the Tb^{3+} sublattice. P_{III}^y is linear in the temperature which matches the increase of ordered magnetic moment of the Tb^{3+} ions below 10 K [14, 15, 24, 25].

The field dependence of the magnetic Tb^{3+} order and of $P_{III}^y(H_x)$, expressed by Fig. 3 and Eq. (9), points to the competition of two independent mechanisms to the magnetoelectric response. On the one hand, we have $P_{III,AFM}^y(H_x)$, which is related to the long-range ordered AFM component of the rare-earth sublattice. This is the only contribution present at $H_x = 0$. At $H_x \neq 0$ this polarization is *diminished* by the fraction of the magnetic rare-earth moment that is paramagnetically aligned along x [8]. This is expressed by $P_{III,AFM}^y(H_x) = P_{III,AFM}^y(0) - \beta_1 M_x^2$ with M_x as paramagnetic magnetization and β_1 determined by $\lim_{H_x \rightarrow \infty} P_{III,AFM}^y(H_x) = 0$. On the other hand, we have $P_{III,PM}^y(H_x)$, which is the polarization *induced* by the paramagnetically aligned component of the rare-earth moments. This is expressed by $P_{III,PM}^y(H_x) = \beta_2 M_x^2$ with β_2 as susceptibility parametrizing this quadratic magnetoelectric effect [26, 27].

We note that $P_{III,AFM}^y$ is due to the internal exchange interactions involving a scalar product of the Tb^{3+} moments, whereas $P_{III,PM}^y(H_x)$ is related to the product of the magnetic moment vector and the external magnetic field inducing M_x .

Since both the AFM demagnetization and the quadratic magnetoelectric effect depend quadratically on the paramagnetic magnetization, the two contributions are jointly described by the coefficient $\beta = \beta_1 + \beta_2$ in Eq. (9). The paramagnetic behaviour is reflected by the Brillouin function fitting $M_x(H_x)$ in Fig. 3 [3, 26]. Note that beyond about ± 3 T the quadratic magnetoelectric contribution exceeds the remaining AFM contribution to the polarization so that the change of sign of P_{III}^y occurs. Furthermore, $P_{III,PM}^y(H_x)$ persists up to temperatures $T > T_5$ [3, 7], which once more emphasizes its relation to the paramagnetic magnetization (in contrast to the AFM long-range Tb^{3+} order disappearing at T_5).

The quadratic dependence of P_{III}^y on the magnetic field in Eq. (9) can be understood in two ways. Macroscopically, it expresses that the magnetoelectric polar-

ization does not depend on the sign of H_x , which is also in agreement with symmetry considerations. Microscopically, it expresses the relation of the magnetoelectric polarization to the isotropic $\text{Tb}^{3+}\text{-Tb}^{3+}$ exchange.

The SHG data reveal further clues about the microscopic origin of P_{III}^y : On the one hand, SHG probes the $\text{Mn} \rightarrow \text{O}$ charge-transfer excitation [9, 28] and can thus be sensitive to the magnetic $\text{Mn}^{3+/4+}$ order and the related polarization $P_{I,II}^y$. On the other hand, SHG couples to the Tb^{3+} -related polarization P_{III}^y although optical Tb^{3+} excitations are not present in the range where the SHG data were taken. This relates P_{III}^y to an exchange interaction between the Tb^{3+} and the $\text{Mn}^{3+/4+}$ spins. However the SHG data *do not* simply reproduce the magnetic moment exerted onto the $\text{Mn}^{3+/4+}$ ions by the ordered Tb^{3+} spins, as this would also affect P_I^y and P_{II}^y . This inevitably leads to the oxygen as only other ingredient involved in the $\text{Tb}^{3+}\text{-Mn}^{3+/4+}$ exchange coupling. We thus propose that P_{III}^y originates in O^{2-} ions that are spin-polarized by the Tb^{3+} long-range order and therefore affect the $\text{Mn} \rightarrow \text{O}$ charge transfer probed by SHG. Recent results showing the importance of spin-polarized oxygen for the ferroelectric properties of RMn_2O_5 support this conclusion [29, 30].

VIII. CONCLUSIONS

Three independent contributions to the magnetically induced spontaneous polarization of multiferroic

TbMn_2O_5 were separated by SHG. All three display a temperature-dependent behaviour in accordance with Landau theory. Two contributions, P_I^y and P_{II}^y , are related to the magnetic $\text{Mn}^{3+/4+}$ order; they were also observed in YMn_2O_5 without rare-earth magnetism. They are insensitive to a magnetic field $\mu_0 H_x$ of up to ± 7 T within 1% of the maximal polarization value. The third contribution, P_{III}^y , is induced by the AFM long-range order of the Tb^{3+} moments, as deduced from the observed temperature and magnetic-field dependence of $P_{III}^y(T, H_x)$. Suppression of this rare-earth order and the emergence of a paramagnetic magnetization in a magnetic field H_x lead to the change of sign of P_{III}^y in TbMn_2O_5 . Our data reveal isotropic $\text{Tb}^{3+}\text{-Tb}^{3+}$ exchange and spin polarized oxygen as likely mechanism behind the rare-earth-induced ferroelectric contribution.

ACKNOWLEDGMENTS

The authors thank K. Kohn and V.A. Sanina for providing the TbMn_2O_5 single crystals and P. Tolédano for many fruitful discussions. Financial support by the SFB 608 of the DFG is appreciated. R.V.P. acknowledges support by the RFBR project 09-02-00070. The work at Rutgers was supported by National Science Foundation DMR-1104484.

* manfred.fiebig@mat.ethz.ch

-
- [1] R. E. Newnham, J. J. Kramer, W. A. Schulze, and L. E. Cross, *Magnetoferroelectricity in Cr_2BeO_4* , J. Appl. Phys. **49**, 6088 (1978).
 - [2] T. Kimura, T. Goto, H. Shintani, K. Ishizaka, T. Arima, and Y. Tokura, *Magnetic control of ferroelectric polarization*, Nature (London) **426**, 55 (2003).
 - [3] N. Hur, S. Park, P. Sharma, J. Ahn, S. Guha, and S.-W. Cheong, *Electric polarization reversal and memory in a multiferroic material induced by magnetic fields*, Nature (London) **429**, 392 (2004).
 - [4] S.-W. Cheong and M. Mostovoy, *Multiferroics: a magnetic twist for ferroelectricity*, Nature Mater. **6**, 13 (2007).
 - [5] C. Jia, S. Onoda, N. Nagaosa, and J. H. Han, *Microscopic theory of spin-polarization coupling in multiferroic transition metal oxides*, Phys. Rev. B **76**, 144424 (2007).
 - [6] T. Arima, *Ferroelectricity Induced by Proper-Screw Type Magnetic Order*, J. Phys. Soc. Jpn. **76**, 073702 (2007).
 - [7] Y.S. Oh, B.G. Jeon, S.Y. Haam, S. Park, V.F. Correa, A.H. Lacerda, S.W. Cheong, G.S. Jeon, and K.H. Kim, *Strong magnetoelastic effect on the magnetoelectric phenomena of TbMn_2O_5* , Phys. Rev. B **83**, 060405 (2011).
 - [8] R.D. Johnson, C. Mazzoli, S.R. Bland, C.H. Du, and P.D. Hatton, *Magnetically induced electric polarization reversal in multiferroic TbMn_2O_5 : Terbium spin reorientation studied by resonant x-ray diffraction*, Phys. Rev. B **83**, 054438 (2011).
 - [9] Th. Lottermoser, D. Meier, R.V. Pisarev, and M. Fiebig, *Giant coupling of second-harmonic generation to multiferroic polarization*, Phys. Rev. B **80**, 100101(R) (2009).
 - [10] P. Tolédano, W. Schranz, and G. Krexner, *Induced ferroelectric phases in TbMn_2O_5* , Phys. Rev. B **79**, 144103 (2009).
 - [11] V.V. Menshenin, *Interrelation between the soliton lattice and electric polarization in RMn_2O_5 oxides*, JETP **108**, 236 (2009).
 - [12] J.-C. Toledano and P. Toledano, *The Landau theory of phase transitions* (World Scientific Publishing Co. Pte. Ltd., 1987).
 - [13] I. Kagomiya, K. Kohn, and T. Uchiyama, *Structure and Ferroelectricity of RMn_2O_5* , Ferroelectrics **280**, 131 (2002).
 - [14] S. Kobayashi, T. Osawa, H. Kimura, Y. Noda, N. Kasahara, S. Mitsuda, and K. Kohn, *Neutron Diffraction Study of Successive Magnetic Phase Transitions in Ferroelectric TbMn_2O_5* , J. Phys. Soc. Jpn. **73**, 3439 (2004).
 - [15] R.D. Johnson, S.R. Bland, C. Mazzoli, T.A.W. Beale, C.H. Du, C. Detlefs, S.B. Wilkins, and P.D. Hatton, *Determination of magnetic order of the rare-earth ions in multiferroic TbMn_2O_5* , Phys. Rev. B **78**, 104407 (2008).
 - [16] Y. Shen, *The Principles of Nonlinear Optics* (John Wiley & Sons, 2002).

- [17] M. Fiebig, V.V. Pavlov, and R.V. Pisarev, *Second-harmonic generation as a tool for studying electronic and magnetic crystals: review*, J. Opt. Soc. Am. B **22**, 96 (2005).
- [18] Y. Uesu, S. Kurimura, and Y. Yamamoto, *New nonlinear optical microscope and its application to the observation of ferroelectric domain structure*, Ferroelectrics **169**, 249 (1995).
- [19] C.R. dela Cruz, B. Lorenz, Y.Y. Sun, Y. Wang, S. Park, S.W. Cheong, M.M. Gospodinov, and C.W. Chu, *Pressure-induced enhancement in multiferroic RMn_2O_5 ($R=Tb, Dy, Ho$)*, Phys. Rev. B **76**, 174106 (2007).
- [20] P. Radaelli and L. Chapon, *A neutron diffraction study of RMn_2O_5 multiferroics*, J. Phys.: Condens. Matter **20**, 434213 (2008).
- [21] M. Fukunaga and Y. Noda, *Classification and Interpretation of the Polarization of Multiferroic RMn_2O_5* , J. Phys. Soc. Jpn. **79**, 054705 (2010).
- [22] C. Wehrenfennig, D. Meier, Th. Lottermoser, T. Lonkai, J.-U. Hoffmann, N. Aliouane, D. N. Argyriou, and M. Fiebig, *Incompatible magnetic order in multiferroic hexagonal $DyMnO_3$* , Phys. Rev. B **82**, 100414 (2010).
- [23] G.R. Blake, L.C. Chapon, P.G. Radaelli, S. Park, N. Hur, S.W. Cheong, and J. Rodríguez-Carvajal, *Spin structure and frustration in multiferroic RMn_2O_5 ($R = Tb, Ho, Dy$)*, Phys. Rev. B **71**, 214402 (2005).
- [24] J. Koo, C. Song, S. Ji, J.-S. Lee, J. Park, T.-H. Jang, C.-H. Yang, J.-H. Park, Y. Jeong, K.-B. Lee, *Non-Resonant and Resonant X-Ray Scattering Studies on Multiferroic $TbMn_2O_5$* , et al., Phys. Rev. Lett. **99**, 197601 (2007).
- [25] L.C. Chapon, G.R. Blake, M.J. Gutmann, S. Park, N. Hur, P.G. Radaelli, and S.W. Cheong, *Structural Anomalies and Multiferroic Behavior in Magnetically Frustrated $TbMn_2O_5$* , Phys. Rev. Lett. **93**, 177402 (2004).
- [26] K. Saito and K. Kohn, *Magnetolectric effect and low-temperature phase transitions of $TbMn_2O_5$* , J. Phys. Soc. Jpn. **7**, 2855 (1995).
- [27] H. Nakamura and K. Kohn, *Magnetolectric Effect of Rare Earth Manganese Oxide RMn_2O_5* , Ferroelectrics **204**, 107 (1997).
- [28] A.S. Moskvin and R.V. Pisarev, *Charge-transfer in mixed-valent multiferroic $TbMn_2O_5$* , Phys. Rev. B **77**, 060102(R) (2008).
- [29] T. Beale, S. Wilkins, R. Johnson, S. Bland, Y. Joly, T. Forrest, D. McMorrow, F. Yakhou, D. Prabhakaran, A. Boothroyd, *Antiferromagnetically spin polarized oxygen in magneto-electric $TbMn_2O_5$* , et al., Phys. Rev. Lett. **105**, 087203 (2010).
- [30] S. Partzsch, S. B. Wilkins, J. P. Hill, E. Schierle, E. Weschke, D. Souptel, B. Büchner, and J. Geck, *Observation of Electronic Ferroelectric Polarization in Multiferroic YMn_2O_5* , Phys. Rev. Lett. **107**, 057201 (2011).